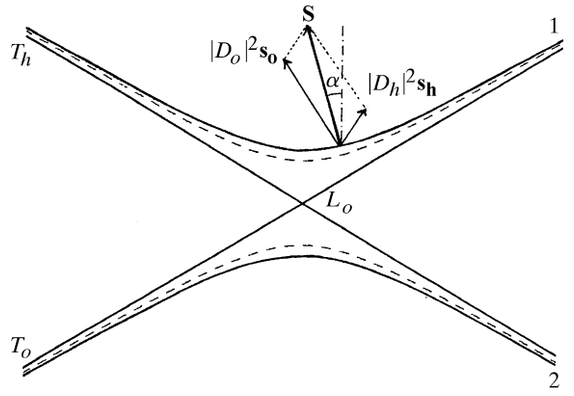

Fig. 5.1.2.5. Dispersion surface for the two states of polarization. Solid curve: polarization normal to the plane of incidence ($C = 1$); broken curve: polarization parallel to the plane of incidence ($C = \cos 2\theta$). The direction of propagation of the energy of the wavefields is along the Poynting vector, **S**, normal to the dispersion surface.

$$\overline{A_{o2}A_{o1}} = |C|R\lambda(F_hF_{\bar{h}})^{1/2}/(\pi V\cos\theta). \qquad (5.1.2.23)$$

It can be noted that the larger the diameter of the dispersion surface, the larger the structure factor, that is, the stronger the interaction of the waves with the matter. When the polarization is parallel to the plane of incidence ($C = \cos 2\theta$), the interaction is weaker.

The asymptotes T_o and T_h to the hyperbola are tangents to the circles centred at O and H, respectively. Their intersection, L_o, is called the *Lorentz point* (Fig. 5.1.2.4).

A wavefield propagating in the crystal is characterized by a tie point P on the dispersion surface and two waves with wavevectors $\mathbf{K_o} = \mathbf{OP}$ and $\mathbf{K_h} = \mathbf{HP}$, respectively. The ratio, ξ, of their amplitudes D_h and D_o is given by means of (5.1.2.20):

$$\xi = \frac{D_h}{D_o} = \frac{2X_o}{kC\chi_{\bar{h}}} = \frac{-2\pi VX_o}{R\lambda CF_{\bar{h}}}. \qquad (5.1.2.24)$$

The hyperbola has two branches, 1 and 2, for each direction of polarization, that is, for $C = 1$ or $\cos 2\theta$ (Fig. 5.1.2.5). Branch 2 is the one situated on the same side of the asymptotes as the reciprocal-lattice points O and H. Given the orientation of the wavevectors, which has been chosen away from the reciprocal-lattice points (Fig. 5.1.2.1*b*), the coordinates of the tie point, X_o and X_h, are positive for branch 1 and negative for branch 2. The phase of ξ is therefore equal to $\pi + \varphi_h$ and to φ_h for the two branches, respectively, where φ_h is the phase of the structure factor [equation (5.1.2.6)]. This difference of π between the two branches has important consequences for the properties of the wavefields.

As mentioned above, owing to absorption, wavevectors are actually complex and so is the dispersion surface (see Authier, 2008).

5.1.2.6. Propagation direction

The energy of all the waves in a given wavefield propagates in a common direction, which is given by that of the Poynting vector (von Laue, 1952) [see Section A5.1.1.4, equation (A5.1.1.8) of the Appendix]. It can be shown that, averaged over time and the unit cell, the Poynting vector of a wavefield is

$$\mathbf{S} = (c/\varepsilon_0)\exp(4\pi\mathbf{K_{oi}}\cdot\mathbf{r})\big[|D_o|^2\mathbf{s_o} + |D_h|^2\mathbf{s_h}\big], \qquad (5.1.2.25)$$

where $\mathbf{s_o}$ and $\mathbf{s_h}$ are unit vectors in the $\mathbf{K_o}$ and $\mathbf{K_h}$ directions, respectively, c is the velocity of light and ε_0 is the dielectric permittivity of a vacuum.

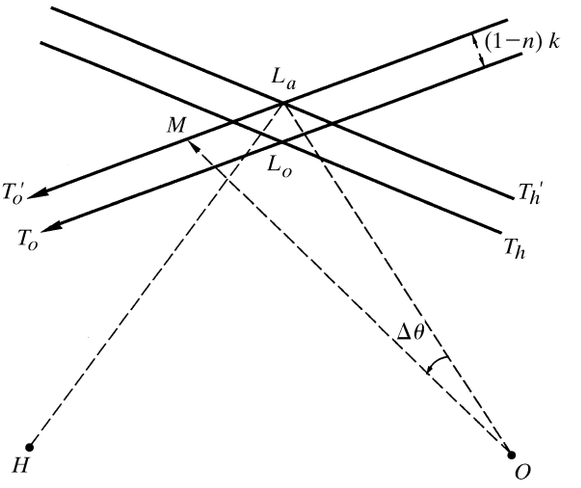

Fig. 5.1.3.1. Departure from Bragg's law of an incident wave.

From (5.1.2.25) and equation (5.1.2.22) of the dispersion surface, it can be shown that the propagation direction of the wavefield lies along the normal to the dispersion surface at the tie point (Fig. 5.1.2.5). This result was first shown by Kato (1952) in the two-beam case for electron diffraction and generalized by him to the n-beam case for X-rays (Kato, 1958). It is also obtained by considering the group velocity of the wavefield (Ewald, 1958; Wagner, 1959). The angle α between the propagation direction and the lattice planes is given by

$$\tan\alpha = \big[(1 - |\xi|^2)/(1 + |\xi|^2)\big]\tan\theta. \qquad (5.1.2.26)$$

It should be noted that the propagation direction varies between $\mathbf{K_o}$ and $\mathbf{K_h}$ for both branches of the dispersion surface.

5.1.3. Solutions of plane-wave dynamical theory

5.1.3.1. Departure from Bragg's law of the incident wave

The wavefields excited in the crystal by the incident wave are determined by applying the boundary condition mentioned above for the continuity of the tangential component of the wavevectors (Section 5.1.2.3). Waves propagating in a vacuum have wavenumber $k = 1/\lambda$. Depending on whether they propagate in the incident or in the reflected direction, the common extremity, M, of their wavevectors

$$\mathbf{OM} = \mathbf{K_o^{(a)}} \text{ and } \mathbf{HM} = \mathbf{K_h^{(a)}}$$

lies on spheres of radius k and centred at O and H, respectively. The intersections of these spheres with the plane of incidence are two circles which can be approximated by their tangents T_o' and T_h' at their intersection point, L_a, or *Laue point* (Fig. 5.1.3.1).

Bragg's condition is exactly satisfied according to the geometrical theory of diffraction when M lies at L_a. The departure $\Delta\theta$ from Bragg's incidence of an incident wave is defined as the angle between the corresponding wavevectors **OM** and $\mathbf{OL}_a$. As $\Delta\theta$ is very small compared to the Bragg angle in the general case of X-rays or neutrons, one may write

$$\begin{aligned}\mathbf{K_o^{(a)}} &= \mathbf{OM} = \mathbf{OL}_a + \mathbf{L}_a\mathbf{M},\\ \Delta\theta &= \overline{L_aM}/k.\end{aligned} \qquad (5.1.3.1)$$

The tangent T_o' is oriented in such a way that $\Delta\theta$ is negative when the angle of incidence is smaller than the Bragg angle.

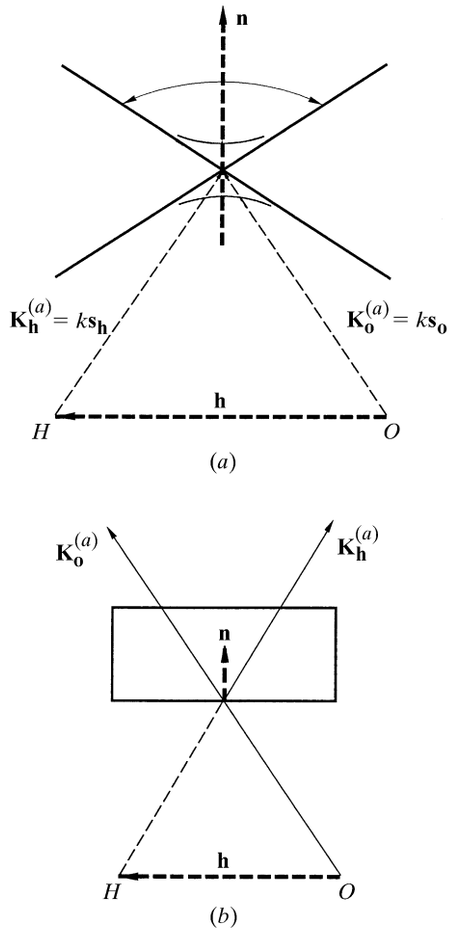

Fig. 5.1.3.2. Transmission, or Laue, geometry. (*a*) Reciprocal space; (*b*) direct space.

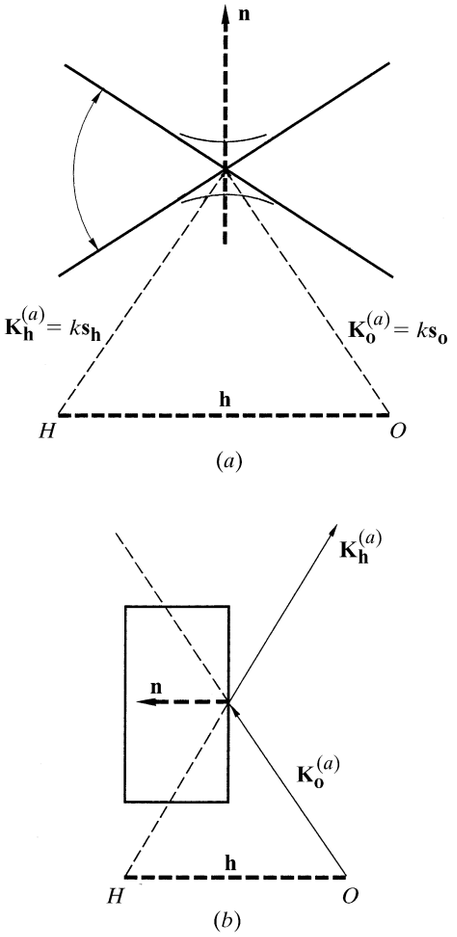

Fig. 5.1.3.3. Reflection, or Bragg, geometry. (*a*) Reciprocal space; (*b*) direct space.

5.1.3.2. Transmission and reflection geometries

The boundary condition for the continuity of the tangential component of the wavevectors is applied by drawing from M a line, **Mz**, parallel to the normal **n** to the crystal surface. The tie points of the wavefields excited in the crystal by the incident wave are at the intersections of this line with the dispersion surface. Two different situations may occur:

(*a*) *Transmission, or Laue case* (Fig. 5.1.3.2). The normal to the crystal surface drawn from M intersects *both* branches of the dispersion surface (Fig. 5.1.3.2*a*). The reflected wave is then directed towards the *inside* of the crystal (Fig. 5.1.3.2*b*). Let γ_o and γ_h be the cosines of the angles between the normal to the crystal surface, **n**, and the incident and reflected directions, respectively:

$$\gamma_o = \cos(\mathbf{n}, \mathbf{s_o}); \quad \gamma_h = \cos(\mathbf{n}, \mathbf{s_h}). \tag{5.1.3.2}$$

It will be noted that they are both positive, as is their ratio,

$$\gamma = \gamma_h/\gamma_o. \tag{5.1.3.3}$$

This is the *asymmetry ratio*, which is very important since the width of the rocking curve is proportional to its square root [equation (5.1.3.6)].

(*b*) *Reflection, or Bragg case* (Fig. 5.1.3.3). In this case there are three possible situations: the normal to the crystal surface drawn from M intersects either branch 1 or branch 2 of the dispersion surface, or the intersection points are imaginary (Fig. 5.1.3.3*a*). The reflected wave is directed towards the *outside* of the crystal (Fig. 5.1.3.3*b*). The cosines defined by (5.1.3.2) are now positive for γ_o and negative for γ_h. The asymmetry factor is therefore also negative.

5.1.3.3. Middle of the reflection domain

It will be apparent from the equations given later that the incident wavevector corresponding to the middle of the reflection domain is, in both cases, **OI**, where I is the intersection of the normal to the crystal surface drawn from the Lorentz point, L_o, with T_o' (Figs. 5.1.3.4 and 5.1.3.5), while, according to Bragg's law, it should be $\mathbf{OL}_a$. The angle $\Delta\theta$ between the incident wavevectors $\mathbf{OL}_a$ and **OI**, corresponding to the middle of the reflecting domain according to the geometrical and dynamical theories, respectively, is

$$\Delta\theta_o = \overline{L_a I}/k = R\lambda^2 F_o(1-\gamma)/(2\pi V \sin 2\theta). \tag{5.1.3.4}$$

In the Bragg case, the asymmetry ratio γ is negative and $\Delta\theta_o$ is never equal to zero. This difference in Bragg angle between the two theories is due to the refraction effect, which is neglected in geometrical theory. In the Laue case, $\Delta\theta_o$ is equal to zero for symmetric reflections ($\gamma = 1$).

5.1.3.4. Deviation parameter

The solutions of dynamical theory are best described by introducing a reduced parameter called the *deviation parameter*,

$$\eta = (\Delta\theta - \Delta\theta_o)/\delta, \tag{5.1.3.5}$$

where

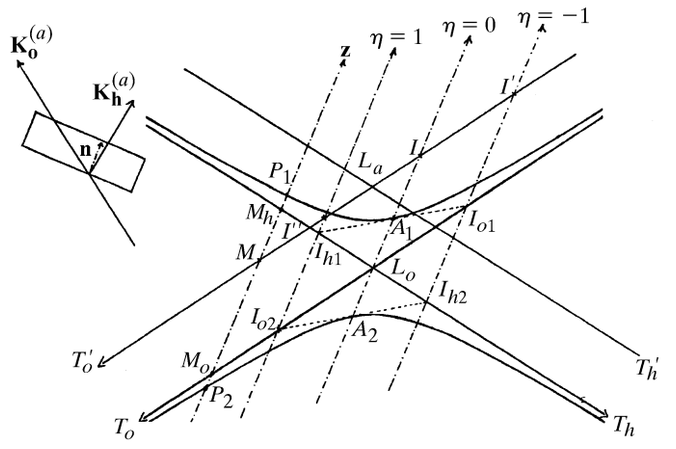

Fig. 5.1.3.4. Boundary conditions at the entrance surface for transmission geometry.

$$\delta = R\lambda^2|C|(|\gamma|F_hF_{\bar{h}})^{1/2}/(\pi V \sin 2\theta), \tag{5.1.3.6}$$

whose real part is equal to the half width of the rocking curve (Sections 5.1.6 and 5.1.7). The width 2δ of the rocking curve is sometimes called the *Darwin width*.

The definition (5.1.3.5) of the deviation parameter is independent of the geometrical situation (reflection or transmission case); this is not followed by some authors. The present convention has the advantage of being quite general.

In an absorbing crystal, η, $\Delta\theta_o$ and δ are complex, and it is the real part, $\Delta\theta_{or}$, of $\Delta\theta_o$ which has the geometrical interpretation given in Section 5.1.3.3. One obtains

$$\begin{aligned}
&\eta = \eta_r + i\eta_i \\
&\eta_r = (\Delta\theta - \Delta\theta_{or})/\delta_r; \;\; \eta_i = A\eta_r + B \\
&A = -\tan\beta \\
&B = \left\{\chi_{io}/\left[|C|(|\chi_h\chi_{\bar{h}}|)^{1/2}\cos\beta\right]\right\}(1-\gamma)/2(|\gamma|)^{1/2},
\end{aligned} \tag{5.1.3.7}$$

where β is the phase angle of $(\chi_h\chi_{\bar{h}})^{1/2}$ [or that of $(F_hF_{\bar{h}})^{1/2}$].

5.1.3.5. Pendellösung and extinction distances

Let

$$\Lambda_o = \pi V(\gamma_o|\gamma_h|)^{1/2}/[R\lambda|C|(F_hF_{\bar{h}})^{1/2}]. \tag{5.1.3.8}$$

This length plays a very important role in the dynamical theory of diffraction by both perfect and deformed crystals. For example, it is 15.3 μm for the 220 reflection of silicon, with Mo $K\alpha$ radiation and a symmetric reflection.

In *transmission* geometry, it gives the period of the interference between the two excited wavefields which constitutes the *Pendellösung* effect first described by Ewald (1917) (see Section 5.1.6.3); Λ_o in this case is called the *Pendellösung distance*, denoted Λ_L hereafter. Its geometrical interpretation, in the zero-absorption case, is the inverse of the diameter A_2A_1 of the dispersion surface in a direction defined by the cosines γ_h and γ_o with respect to the reflected and incident directions, respectively (Fig. 5.1.3.4). It reduces to the inverse of $A_{o2}A_{o1}$ (5.1.2.23) in the symmetric case.

In *reflection* geometry, it gives the absorption distance in the total-reflection domain and is called the *extinction* distance, denoted Λ_B (see Section 5.1.7.1). Its geometrical interpretation in the zero-absorption case is the inverse of the length $I_{o1}I_{h1} = I_{h2}I_{o2}$, Fig. 5.1.3.5.

In a *deformed* crystal, if distortions are of the order of the width of the rocking curve over a distance Λ_o, the crystal is considered to be slightly deformed, and ray theory (Penning & Polder, 1961; Kato, 1963, 1964*a*,*b*) can be used to describe the propagation of wavefields. If the distortions are larger, new wavefields may be generated by interbranch scattering (Authier & Balibar, 1970) and generalized dynamical diffraction theory such as that developed by Takagi (1962, 1969) should be used.

Using (5.1.3.8), expressions (5.1.3.5) and (5.1.3.6) can be rewritten in the very useful form:

$$\begin{aligned}
&\eta = (\Delta\theta - \Delta\theta_o)\Lambda_o \sin 2\theta/(\lambda|\gamma_h|), \\
&\delta = \lambda|\gamma_h|/(\Lambda_o \sin 2\theta).
\end{aligned} \tag{5.1.3.9}$$

The order of magnitude of the Darwin width 2δ ranges from a fraction of a second of an arc to ten or more seconds, and

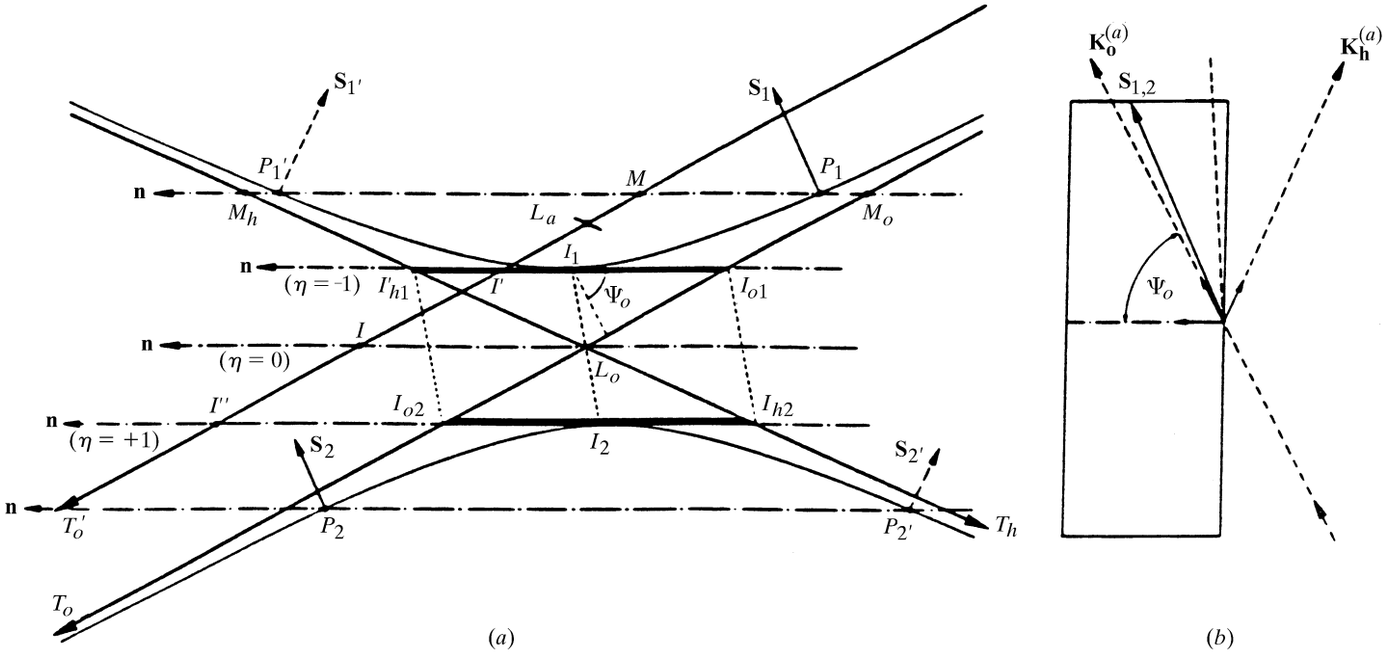

Fig. 5.1.3.5. Boundary conditions at the entrance surface for reflection geometry. (*a*) Reciprocal space; (*b*) direct space.

increases with increasing wavelength and increasing structure factor. For example, for the 220 reflection of silicon and Cu $K\alpha$ radiation, it is 5.2 seconds.

5.1.3.6. Solution of the dynamical theory

The coordinates of the tie points excited by the incident wave are obtained by looking for the intersection of the dispersion surface, (5.1.2.22), with the normal **Mz** to the crystal surface (Figs. 5.1.3.4 and 5.1.3.5). The ratio ξ of the amplitudes of the waves of the corresponding wavefields is related to these coordinates by (5.1.2.24) and is found to be

$$\begin{aligned}\xi_j &= D_{hj}/D_{oj} \\ &= -\mathrm{S}(C)\mathrm{S}(\gamma_h)[(F_hF_{\bar{h}})^{1/2}/F_{\bar{h}}] \\ &\quad\times\left\{\eta \pm \left[\eta^2 + \mathrm{S}(\gamma_h)\right]^{1/2}\right\}/(|\gamma|)^{1/2},\end{aligned} \tag{5.1.3.10}$$

where the plus sign corresponds to a tie point on branch 1 ($j = 1$) and the minus sign to a tie point on branch 2 ($j = 2$), and $\mathrm{S}(\gamma_h)$ is the sign of γ_h (+1 in transmission geometry, −1 in reflection geometry).

5.1.3.7. Geometrical interpretation of the solution in the zero-absorption case

5.1.3.7.1. Transmission geometry

In this case (Fig. 5.1.3.4) $\mathrm{S}(\gamma_h)$ is +1 and (5.1.3.10) may be written

$$\xi_j = -\mathrm{S}(C)\left[\eta \pm (\eta^2 + 1)^{1/2}\right]/\gamma^{1/2}. \tag{5.1.3.11}$$

Let A_1 and A_2 be the intersections of the normal to the crystal surface drawn from the Lorentz point L_o with the two branches of the dispersion surface (Fig. 5.1.3.4). From Sections 5.1.3.3 and 5.1.3.4, they are the tie points excited for $\eta = 0$ and correspond to the middle of the reflection domain. Let us further consider the tangents to the dispersion surface at A_1 and A_2 and let I_{o1}, I_{o2} and I_{h1}, I_{h2} be their intersections with T_o and T_h, respectively. It can be shown that $\overline{I_{o1}I_{h2}}$ and $\overline{I_{o2}I_{h1}}$ intersect the dispersion surface at the tie points excited for $\eta = -1$ and $\eta = +1$, respectively, and that the *Pendellösung* distance $\Lambda_\mathrm{L} = 1/\overline{A_2A_1}$, the width of the rocking curve $2\delta = \overline{I_{o1}I_{o2}}/k$ and the deviation parameter $\eta = \overline{M_oM_h}/\overline{A_2A_1}$, where M_o and M_h are the intersections of the normal to the crystal surface drawn from the extremity of any incident wavevector **OM** with T_o and T_h, respectively.

5.1.3.7.2. Reflection geometry

In this case (Fig. 5.1.3.5) $\mathrm{S}(\gamma_h)$ is now −1 and (5.1.3.10) may be written

$$\xi_j = \mathrm{S}(C)\left[\eta \pm (\eta^2 - 1)^{1/2}\right]/|\gamma|^{1/2}. \tag{5.1.3.12}$$

Now, let I_1 and I_2 be the points of the dispersion surface where the tangent is parallel to the normal to the crystal surface, and further let I_{o1}, I_{h1}, I' and I_{o2}, I_{h2}, I'' be the intersections of these two tangents with T_o, T_h and T'_o, respectively. For an incident wave of wavevector **OM** where M lies between I' and I'', the normal to the crystal surface drawn from M has no real intersection with the dispersion surface and $\overline{I'I''}$ defines the total-reflection domain. The tie points I_1 and I_2 correspond to $\eta = -1$ and $\eta = +1$, respectively, the extinction distance $\Lambda_\mathrm{L} = 1/\overline{I_{o1}I_{h1}}$, the width of the total-reflection domain $2\delta = \overline{I_{o1}I_{o2}}/k = \overline{I'I''}/k$ and the deviation parameter $\eta = -\overline{M_oM_h}/\overline{I_{o1}I_{h1}}$, where M_o and M_h are the intersections with T_o and T_h of the normal to the crystal surface drawn from the extremity of any incident wavevector **OM**.

5.1.4. Standing waves

The various waves in a wavefield are coherent and interfere. In the two-beam case, the intensity of the wavefield, using (5.1.2.14) and (5.1.2.24), is

$$\begin{aligned}|D|^2 &= |D_o|^2 \exp(4\pi\mathbf{K_{oi}}\cdot\mathbf{r}) \\ &\quad\times[1 + |\xi|^2 + 2C|\xi|\cos 2\pi(\mathbf{h}\cdot\mathbf{r} + \Psi)],\end{aligned} \tag{5.1.4.1}$$

where Ψ is the phase of ξ,

$$\xi = |\xi|\exp(i\Psi). \tag{5.1.4.2}$$

Equation (5.1.4.1) shows that the interference between the two waves is the origin of *standing waves*. The corresponding nodes lie on planes such that $\mathbf{h}\cdot\mathbf{r}$ is a constant. These planes are therefore parallel to the diffraction planes and their periodicity is equal to d_{hkl} (defined in the caption for Fig. 5.1.2.1*a*). Their position within the unit cell is given by the value of the phase Ψ.

In the Laue case, Ψ is equal to $\pi + \varphi_h$ for branch 1 and to φ_h for branch 2, where φ_h is the phase of the structure factor, (5.1.2.6). This means that the *nodes* of standing waves lie on the maxima of the *hkl* Fourier component of the electron density for branch 1 while the *anti-nodes* lie on the maxima for branch 2.

In the Bragg case, Ψ varies continuously from $\pi + \varphi_h$ to φ_h as the angle of incidence is varied from the low-angle side to the high-angle side of the reflection domain by rocking the crystal. The nodes lie on the maxima of the *hkl* Fourier components of the electron density on the low-angle side of the rocking curve. As the crystal is rocked, they are progressively shifted by half a lattice spacing until the anti-nodes lie on the maxima of the electron density on the high-angle side of the rocking curve.

Standing waves are the origin of the phenomenon of anomalous absorption, which is one of the specific properties of wavefields (Section 5.1.5). Anomalous scattering is also used for the location of atoms in the unit cell at the vicinity of the crystal surface: when X-rays are absorbed, fluorescent radiation and photoelectrons are emitted. Detection of this emission for a known angular position of the crystal with respect to the rocking curve and therefore for a known value of the phase Ψ enables the emitting atom within the unit cell to be located. The principle of this method is due to Batterman (1964, 1969). For reviews, see Golovchenko *et al.* (1982), Materlik & Zegenhagen (1984), Kovalchuk & Kohn (1986), Bedzyk (1988), Authier (1989), Zegenhagen (1993), Patel (1996), Patel & Fontes (1996), Lagomarsino (1996), Zegenhagen *et al.* (1997), Vartanyants & Zegenhagen (1999) and Vartanyants & Koval'chuk (2001).

5.1.5. Anomalous absorption

It was shown in Section 5.1.2.2 that the wavevectors of a given wavefield all have the same imaginary part (5.1.2.17) and therefore the same absorption coefficient μ (5.1.2.19). Borrmann (1950, 1954) showed that this coefficient is much smaller than the normal one (μ_o) for wavefields whose tie points lie on branch 1 of the dispersion surface and much larger for wavefields whose tie points lie on branch 2. The former case corresponds to the *anomalous transmission effect*, or *Borrmann effect*. As in favourable cases the minimum absorption coefficient may be as low as a few per cent of μ_o, this effect is very important from both a fundamental and a practical point of view.

The physical interpretation of the Borrmann effect is to be found in the standing waves described in Section 5.1.4. When the